Formation and Interaction of Membrane Tubes

Imre Derényi,[1,2] Frank Jülicher,[1,3] and Jacques Prost[1]

[1]*Institut Curie, UMR 168, 26 rue d'Ulm, F-75248 Paris Cédex 05, France*
[2]*Department of Biological Physics, Eötvös University, Pázmány P. stny. 1A, H-1117 Budapest, Hungary*
[3]*Max Planck Institut für Physik komplexer Systeme, Nöthnitzer Strasse 38, D-01187 Dresden, Germany*
(Received 8 February 2002; published 28 May 2002)

We show that the formation of membrane tubes (or membrane tethers), which is a crucial step in many biological processes, is highly nontrivial and involves first-order shape transitions. The force exerted by an emerging tube is a nonmonotonic function of its length. We point out that tubes attract each other, which eventually leads to their coalescence. We also show that detached tubes behave like semiflexible filaments with a rather short persistence length. We suggest that these properties play an important role in the formation and structure of tubular organelles.

Biological membranes (such as the endoplasmic reticulum, the Golgi apparatus, the inner mitochondrial membrane, or the plasma membrane) often form highly dynamic tubular networks [1]. The formation and transport of membrane tubes (tens of nanometers in diameter) are thought to involve motor proteins that are able to grab the membrane and pull on it as they move along the filaments of the cytoskeleton [2]. Nanotubes (or tethers) can also be pulled out by various experimental techniques (such as hydrodynamic flow [3], micropipettes [4], or optical tweezers [5]), and very recently Roux *et al.* [6] have managed to set up a minimal *in vitro* experimental system, in which tubes have been pulled by kinesin motor proteins. The physics of long tubular membranes is relatively simple and is well understood. However, the initial formation of nanotubes from planar or large spherical pieces of membrane is a subtle process, the understanding of which is crucial to the study of various biological processes (involving tube formation or simply membrane pulling). In addition to tube formation we also study the interaction of membrane tubes pulled from the same membrane, and make a few comments on the mechanical properties of detached membrane tubes.

Living cells maintain the surface tension of most of their membranes at a constant level by keeping lipid reservoirs (at fixed chemical potentials) [5]. A constant pressure in closed vesicles is also maintained via osmosis. Therefore, for our study we choose the ensemble in which the surface tension σ and the inside pressure p (relative to the outside) are fixed rather than the surface area of the membrane A or the volume of the vesicle V.

With the bending term included the free energy of the membrane can be written as [7]

$$\mathcal{F} = \int \frac{\kappa}{2}(2H)^2 \, dA + \sigma A - pV - fL, \quad (1)$$

where κ is the bending rigidity and H is the mean curvature of the membrane. The membrane is pulled in the Z direction with a point force f, and the end-to-end distance of the membrane in this direction is denoted by L.

For a tube of length L and radius R the free energy (at $p = 0$) can be written as $\mathcal{F}_{\text{tube}} = [\kappa/(2R^2) + \sigma]2\pi RL - fL$. To minimize $\mathcal{F}_{\text{tube}}$ the surface tension acts to reduce the radius, while the bending rigidity works against this. The balance between the two sets the equilibrium radius R_0 and force f_0, which can be calculated by taking $\partial \mathcal{F}_{\text{tube}}/\partial R = 0$ and $\partial \mathcal{F}_{\text{tube}}/\partial L = 0$:

$$R_0 = \sqrt{\frac{\kappa}{2\sigma}}, \qquad f_0 = 2\pi\sqrt{2\sigma\kappa}. \quad (2)$$

For typical values of $\kappa \approx 40$ pN nm and $\sigma \approx 0.05$ pN/nm, one finds $R_0 \approx 20$ nm and $f_0 \approx 12.6$ pN.

For simplicity we consider only axisymmetric surfaces with the Z axis being the symmetry axis (Fig. 1a, upper inset). Such surfaces can be parametrized by the angle $\psi(S)$, where S is the arclength along the contour. The coordinates $R(S)$ and $Z(S)$ depend on $\psi(S)$ through

$$\dot{R} = \cos\psi, \qquad \dot{Z} = -\sin\psi, \quad (3)$$

and the mean curvature can be expressed as

$$2H = \dot{\psi} + (\sin\psi)/R. \quad (4)$$

For axisymmetric surfaces, one can derive the so-called general shape equation from the free energy (1) by variational methods [8,9]:

$$\dddot{\psi} = -\frac{1}{2}\dot{\psi}^3 - \frac{2\cos\psi}{R}\ddot{\psi} + \frac{3\sin\psi}{2R}\dot{\psi}^2 + \frac{3\cos^2\psi - 1}{2R^2}\dot{\psi}$$
$$+ \bar{\sigma}\dot{\psi} - \frac{\cos^2\psi + 1}{2R^3}\sin\psi + \frac{\bar{\sigma}}{R}\sin\psi - \bar{p}, \quad (5)$$

where $\bar{\sigma} = \sigma/\kappa = 1/(2R_0^2)$ and $\bar{p} = p/\kappa$. Taking the first integral of this equation leads to [9]

$$\ddot{\psi}\cos\psi = -\frac{1}{2}\dot{\psi}^2\sin\psi - \frac{\cos^2\psi}{R}\dot{\psi} + \frac{\cos^2\psi + 1}{2R^2}\sin\psi$$
$$+ \bar{\sigma}\sin\psi - \frac{1}{2}\bar{p}R - \frac{\tilde{f}}{R}, \quad (6)$$

with the integration constant $\tilde{f} = f/(2\pi\kappa) = f/(f_0 R_0)$.

For nearly flat membranes ($\psi \ll 1$), after the parameter change $[\psi(S), R(S)] \rightarrow \psi(R)$, one can expand the shape
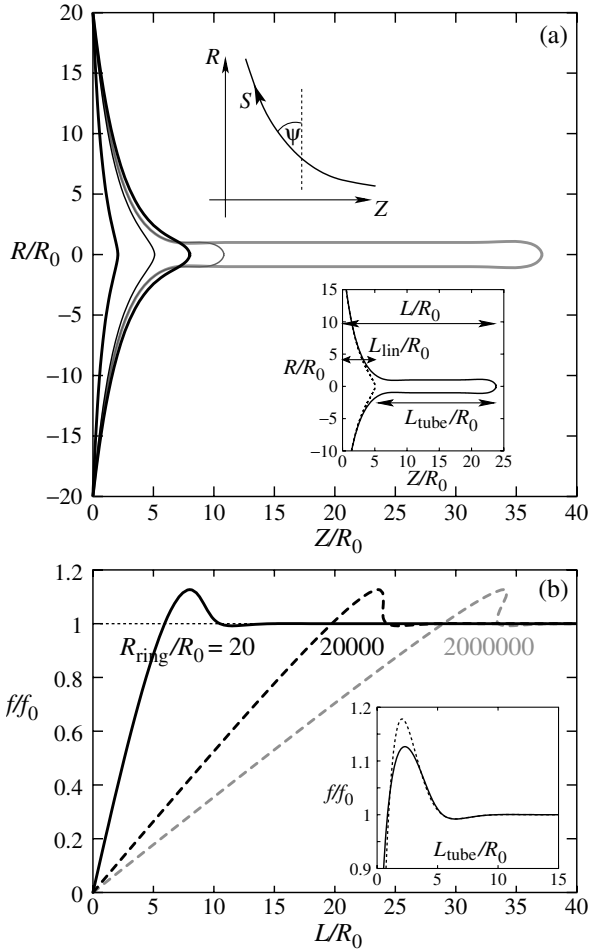
FIG. 1. (a) The shape of an emerging tube at various lengths. The upper inset shows the parametrization of the surface, and the lower inset illustrates the definition of L_{tube}, which is the size of the deviation of the shape from the linear approximation (dashed line). (b) Force vs length curves for three different ring sizes. The inset shows the f-L_{tube} curve (solid line) and its asymptotic fit by Eq. (13) (dashed line).

equation (6) in powers of ψ and keep only the terms up to linear order:

$$R^2\psi'' + R\psi' - (R^2\bar{\sigma} + 1)\psi = -\tilde{f}R - \bar{p}R^3/2. \quad (7)$$

Because of the parameter change, the primes denote derivations with respect to R (which, in linear order of ψ, are identical to derivations with respect to S). The general solution of this differential equation is

$$\psi(R) = \frac{\tilde{f}}{\bar{\sigma}}\frac{1}{R} + \frac{1}{2}\frac{\bar{p}}{\bar{\sigma}}R + c_1 I_1(R\sqrt{\bar{\sigma}}) + c_2 K_1(R\sqrt{\bar{\sigma}}),$$

$$(8)$$

where $I_i(x)$ and $K_i(x)$ are modified Bessel functions, and c_1 and c_2 are integration constants. $I_1(R\sqrt{\bar{\sigma}})$ diverges exponentially for $R \to \infty$. Because for a big vesicle we expect the shape to converge to that of a sphere, c_1 must vanish. At $R = 0$ the divergence of the $1/R$ term must be canceled by the K_1 term, leading to $c_2 = -\tilde{f}/\sqrt{\bar{\sigma}}$. Integrating $-\psi(R)$ with respect to R gives the shape of the membrane in this linear approximation:

$$Z_{lin}(R) = Z_0 - \frac{2R_0 f}{f_0}\left[\ln\left(\frac{R}{\sqrt{2}\,R_0}\right) + K_0\left(\frac{R}{\sqrt{2}\,R_0}\right)\right]$$

$$- \frac{R^2}{2R_{ves}}, \quad (9)$$

where the integration constant Z_0 serves as a reference coordinate, and we have expressed σ, κ, and p in terms of R_0, f_0, and vesicle radius $R_{ves} = 2\sigma/p$. The last term is a trivial contribution, describing a spherical vesicle under tension σ and pressure p. The second term, which is proportional to f, is the linear response, and describes the deformation of the vesicle. The quantity between the brackets converges to $[\ln(2) - \gamma]$ for $R \to 0$, where $\gamma = 0.577,\dots$ is the Euler constant. For $p = 0$ and large R the logarithmic term dominates, which corresponds to a catenoid, the well-known shape of a soap film in cylindrical geometry under zero pressure.

Because the pressure makes only a trivial contribution, and has a negligible effect on tube formation from big vesicles (plug $pR \approx pR_0 = 2\sigma R_0/R_{ves} \ll \sigma$ into the shape equations), we neglect it from now on, and consider a piece of (initially flat) membrane that spans a ring of radius R_{ring} located at $Z = 0$.

For large deformations (or pulling forces) the linear approximation breaks down, and we have to solve Eq. (5) together with Eq. (3) numerically. Note that Eq. (6) could also be used, but it is numerically less stable. We start solving the differential equations from the ring, where we impose a zero curvature (or free hinge) boundary condition. Thus, the four initial parameters at $Z = 0$ are as follows: (i) $R = R_{ring}$; (ii) $\psi = \arcsin[f/(2\pi\sigma R_{ring})] - \varepsilon$, where the small deviation ε from the catenoid shape is chosen (with a shooting and matching technique) such that the contour line reaches the Z axis; (iii) $\dot{\psi} = -(\sin\psi)/R$ ensures zero mean curvature [see Eq. (4)]; (iv) finally, $\ddot{\psi}$ is determined from Eq. (6).

The results of the numerical solution can be seen in Fig. 1. The main part of Fig. 1a shows the shape (contour line) of the membrane for $R_{ring} = 20R_0$ and different values of L. For small deformations (left line) Eq. (9) gives a very good approximation of the shape. In this linear regime the size of the deformation is approximately $L_{lin} = Z_{lin}(0) - Z_{lin}(R_{ring})$.

For larger deformations a tube emerges in the middle, and the linear approximation fails. However, far from the tubular part, where ψ is small, the approximation is still valid (Fig. 1a lower inset). Thus, it is convenient to define the tube as the piece between L_{lin} and L, and the base as the rest of the membrane between 0 and L_{lin}. This way, the dependence of the size of the total deformation L on the ring radius R_{ring} is absorbed in the size of the base L_{lin}, and the length of the tube $L_{tube} = L - L_{lin}$ (i.e., the deviation from the linear approximation) becomes independent of R_{ring}.

With this definition it is enough to determine the f-L curve for one particular ring size (e.g., $20R_0$), from which

the universal (ring-size-independent) f-L_{tube} curve can be calculated (Fig. 1b, inset). Because only the f-L curves have real physical meaning, one can easily calculate them from the f-L_{tube} curve for any ring radius ($\gg R_0$) by simply adding $L_{lin}(f, R_{ring})$ to L_{tube}. The most intriguing feature of the f-L curves (shown in Fig. 1b for three different values of R_{ring}) is their nonmonotonicity. The force first grows linearly, in accordance with the linear approximation (9), and converges to f_0 for large L. But in between it overshoots by $\sim 0.13 f_0$, and then oscillates about f_0 with an exponentially decaying amplitude. This oscillation results in infinitely many intervals with negative slopes, which, in the f ensemble (where f is the control parameter rather than L), are mechanically unstable and represent an infinite series of *first-order shape transitions* at f_0. Because L_{lin} is a monotonically increasing function of both f and R_{ring}, the main peak becomes an overhang for large rings ($>20\,000 R_0$), leading to a first-order transition even in the L ensemble.

For a nearly cylindrical section, such as tubular part of the membrane, the shape equations can be expanded in powers of $U(Z) = R(Z) - R_0$. After changing parameters $[\psi(S), Z(S)] \rightarrow \psi(Z)$, the expansion of Eq. (5) up to first order in $U(Z)$ and for $p = 0$ reduces to [10]

$$R_0^4 U'''' = -U. \tag{10}$$

Here the primes denote derivations with respect to Z. The solution of this equation is the sum of two exponentially decaying oscillations from the two ends (L_{lin} and L) of the tube:

$$\frac{U(Z)}{R_0} = a_1 \exp\left(-\frac{Z - L_{lin}}{\sqrt{2} R_0}\right) \cos\left(\frac{Z - L_{lin}}{\sqrt{2} R_0} + \alpha_1\right)$$
$$+ a_2 \exp\left(-\frac{L - Z}{\sqrt{2} R_0}\right) \cos\left(\frac{L - Z}{\sqrt{2} R_0} + \alpha_2\right), \tag{11}$$

where the integration constants converge to $a_1 \approx 0.746$, $a_2 \approx 0.726$, $\alpha_1 \approx 0.347$, and $\alpha_2 \approx 3.691$ (determined by numerical fitting) as the length of the tube increases. These oscillations can be seen in Fig. 2 as overshootings from
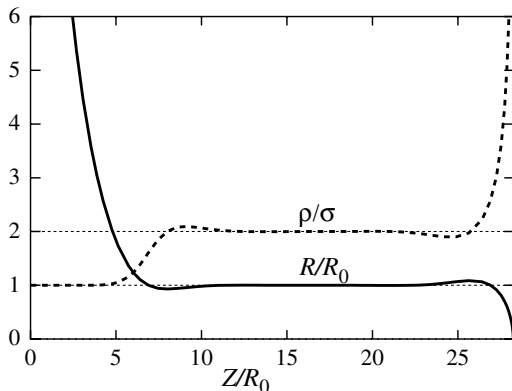

FIG. 2. The shape of a tube magnified in the radial direction (solid line), and the surface energy density (dashed line).

both the base and the tip of the tube. They can be understood intuitively by noticing that the smaller (larger) mean curvature near the base (tip) makes the effect of the bending rigidity on the tube radius less (more) pronounced, leading to a smaller (larger) R.

The expansion of Eq. (6) up to the first nonvanishing order in $U(Z)$ gives us the deviation of the force:

$$\frac{f - f_0}{f_0} = R_0^2 U' U''' - \frac{1}{2} R_0^2 U''^2 + \frac{1}{2} \frac{1}{R_0^2} U^2. \tag{12}$$

Plugging Eq. (11) into Eq. (12) yields

$$\frac{f - f_0}{f_0} = 2 a_1 a_2 \exp\left(-\frac{L_{tube}}{\sqrt{2} R_0}\right) \cos\left(\frac{L_{tube}}{\sqrt{2} R_0} + \alpha_1 + \alpha_2\right), \tag{13}$$

which is an exponentially decaying oscillation as a function of L_{tube}. This explains the observed nonmonotonic behavior of the f-L curves, and gives a very good fit to the f-L_{tube} curve (Fig. 1b, inset) with the same values of a_i and α_i as determined above for the shape oscillations. In a different ensemble, Heinrich *et al.* [11] also observed similar oscillations for axially strained vesicles.

The surface energy density $\rho = (\kappa/2)(2H)^2 + \sigma$ of the membrane is plotted in Fig. 2. It grows from σ to 2σ as we enter the tube from the base, and diverges at the tip. Because at the tip the angle ψ is small again, Eq. (8) can be used to describe the surface there, leading to a logarithmic divergence of the mean curvature [10,12].

In experiments, bundles of tubes can often be observed [6]. To study the interaction between two tubes, let us start with a planar membrane that spans a ring and is pulled perpendicularly by two point forces (f_1 and f_2) at a distance d. If d is large enough ($R_0 \ll d \ll R_{ring}$), both protrusions (except for the vicinity of the points of pulling) can be described by the leading logarithmic term of the linear approximation (9). Their superposition can be used to calculate the d dependence of the free energy of the membrane. Note that fL in Eq. (1) has to be replaced by $f_1 L_1 + f_2 L_2$, where L_1 and L_2 are the sizes of the deformations. A straightforward calculation results in an attractive potential $\mathcal{F}(d) = \text{const} + 2 R_0 \ln(d) f_1 f_2 / f_0$ between the two deformations. The same attraction has been found between membrane-bound adhesion molecules [13]. For the attraction between two tubes, replace both f_1 and f_2 by f_0.

To see what happens when two tubes get close, we performed numerical energy minimization with the SURFACE EVOLVER program [14]. We defined the initial topology as a piece of membrane spanning a ring of radius $12 R_0$ at $Z = 0$, with two cylindrical protrusions in the positive Z direction. We applied a zero curvature boundary condition at the ring and reflecting boundary condition at $Z = 24 R_0$ (Fig. 3). To make sure that the two tubes do not coalesce we placed a very narrow ($\ll R_0$) cylindrical obstacle between the tubes, perpendicularly to them, and at a distance h from the ring (not shown in Fig. 3). The obstacle simply pinned down the middle of the membrane at $Z = h$.
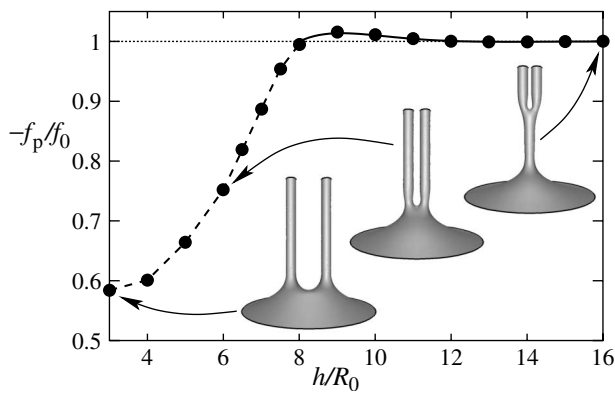
FIG. 3.   The pinning force f_p as a function of h. It goes from $-f_0/2$ (because if two tubes are far apart their attraction can be eliminated by a $-f_0/2$ point force applied halfway) to $-f_0$ (because for large h the junction is pulled by two tubes upward but by only one tube downward). The solid line is a fit by an exponentially decaying oscillation.

We then measured the pinning force f_p (exerted by the obstacle on the membrane) as a function of h. Figure 3 shows that f_p is always negative (i.e., pushes the membrane), meaning that there is no energy barrier against coalescence, it occurs smoothly. This is consistent with the experiments of Evans *et al.* [4].

Tubes can be detached via fission and then transported individually in the cell as long prolatelike vesicles (keeping their original radius R_0). Because of volume and area constraints their energy contains only the bending term: $\mathcal{F} = \int (\kappa/2)(2H)^2 \, dA$. Although with such a high area-to-volume ratio the energetically most favorable shape is the stomatocyte, these prolates are metastable [15]. They are also very flexible. If we consider a prolate as a rod and bend it with a curvature C ($\ll 1/R_0$), its energy, for symmetry reasons, increases quadratically with C. This energy increase can be written as $(\kappa/2)(\lambda C^2)2\pi R_0 L$, where L is the length of the prolate, and the factor $\lambda = \langle \sin^2 \phi \rangle = 1/2$ indicates that, during the integration of the energy around a cross section (parametrized by ϕ), only the out-of-plane component of the bending counts. Thus, the bending stiffness of a prolatelike vesicle is $\kappa \pi R_0$, and its persistence length $\kappa \pi R_0/(k_B T)$ is of the order of a few hundred nanometers.

Although these prolates are thicker than the microtubules, their persistence length is much closer to that of a DNA. This is because their wall is a two-dimensional fluid. Because of this fluidity they do not even resist twisting, which makes them ideal semiflexible filaments.

We close this Letter by discussing some of the biological consequences of our theoretical results. The major biological relevance of the first force peak of the f-L curves is that, in order to form a tube, the motor proteins must be able to provide a force that is 13% larger than what is needed to pull a long tube. At a pulling force of $f = f_0$ the peak corresponds to a $2.1\kappa \approx 21 k_B T$ high energy barrier, which is practically insurmountable for such a big and slow

object as a growing tube. Thus, tube formation works on an all-or-nothing basis: motors can pull out tubes only if they are strong enough to overcome the major force peak.

Although at the tip of the tubes the size of the lipids (~ 0.5 nm) represents a natural cutoff length scale for the divergence of the energy density, it goes up to tens of σ. In terms of membrane rupture, the energy density acts as an effective surface tension, meaning that the most likely place for rupture to occur is the tip of the tubes. So if biological systems want to avoid rupture, they either have to protect the tips or distribute the pulling forces at larger areas. That could be achieved, e.g., by utilizing cap proteins or lipid rafts.

We have shown that without external pinning tubes coalesce smoothly. Thus, to explain bundle formation, other physical effects that could prevent the coalescence of tubes (e.g., adhesion between the tubes and the cytoskeleton) must be taken into account.

[1] C. Lee and L. B. Chen, Cell **54**, 37 (1988); H. H. Mollenhauer and D. J. Morré, Histochem. Cell Biol. **109**, 533 (1998).
[2] S. L. Dabora and M. P. Sheetz, Cell **54**, 27 (1988); N. Hirokawa, Science **279**, 519 (1998); C. M. Waterman-Storer and E. D. Salmon, Curr. Biol. **8**, 798 (1998); A. M. Robertson and V. J. Allan, Mol. Biol. Cell **11**, 941 (2000).
[3] R. E. Waugh, Biophys. J. **38**, 29 (1982).
[4] E. Evans, H. Bowman, A. Leung, D. Needham, and D. Tirrell, Science **273**, 933 (1996).
[5] D. Raucher and M. P. Sheetz, Biophys. J. **77**, 1992 (1999).
[6] A. Roux, G. Cappello, J Cartaud, J. Prost, B. Goud, and P. Bassereau, Proc. Natl. Acad. Sci. U.S.A. **99**, 5394 (2002).
[7] W. Helfrich, Z. Naturforsch. C **28**, 693 (1973); H. J. Deuling and W. Helfrich, J. Phys. (Paris) **37**, 1335 (1976); D. J. Bukman, J. H. Yao, and M. Wortis, Phys. Rev. E **54**, 5463 (1996).
[8] F. Jülicher and U. Seifert, Phys. Rev. E **49**, 4728 (1994); Hu Jian-Guo and Ou-Yang Zhong-Can, Phys. Rev. E **47**, 461 (1993).
[9] W.-M. Zheng and J. Liu, Phys. Rev. E **48**, 2856 (1993); B. Bozic, S. Svetina, and B. Zeks, Phys. Rev. E **55**, 5834 (1997).
[10] B. Bozic, V. Heinrich, S. Svetina, and B. Zeks, Eur. Phys. J. E **6**, 91 (2001).
[11] V. Heinrich, B. Bozic, S. Svetina, and B. Zeks, Biophys. J. **76**, 2056 (1999).
[12] R. Podgornik, S. Svetina, and B. Zeks, Phys. Rev. E **51**, 544 (1995).
[13] D. M. Zuckerman and R. F. Bruinsma, Phys. Rev. E **57**, 964 (1998).
[14] K. Brakke, Exper. Math. **1**, 141 (1992).
[15] U. Seifert, K. Berndl, and R. Lipowsky, Phys. Rev. A **44**, 1182 (1991).